

Determination of Micellar Microenvironment of Pinacyanol by Visible Spectroscopy

Raimon Sabaté and Joan Estelrich*

Departament de Fisicoquímica, Facultat de Farmàcia, Universitat de Barcelona,
Avda. Joan XXIII s/n 08028-Barcelona, Catalonia, Spain

Received: November 7, 2002; In Final Form: February 20, 2003

The interaction of pinacyanol, a cationic cyanine dye (PIN), with Triton X-100, sodium dodecyl sulfate, and alkyltrimethylammonium bromide micelles was studied by visible spectrophotometry. PIN exists as a monomer and in aggregated form (dimers, trimers, and higher aggregates) in aqueous solution, but dimers and higher aggregates were split into monomers in the presence of surfactants (or on addition of organic solvents). The interaction of PIN with any kind of micelles produced a bathochromic shift of all of the spectral bands and increased the most red-shifted band. The deconvolution of each experimental spectrum in three bands allowed the calculation of the molar absorptivity of any band. The extent of the binding of the dye to micelles can be measured by the association constant. The highest value of this was achieved with anionic, then with nonionic, and, finally, with cationic micelles. In the latter, the higher the length of the hydrophobic chain, the higher the association constant. By comparing the wavelength shifts in micellar systems with those observed in organic solvents, it was possible to assign a kind of microenvironment of PIN in the micelle.

1. Introduction

Cyanine dyes are intensively colored, cationic polymethine dyes and have been frequently used as optical probes in the study of membranes, surfactants, micelles, and dendrimer-based host systems.^{1–5} In solution, the main nonradiative relaxation process for the excited singlet state is the rotation around the conjugated polymethine chain.⁶ The quantum yield of fluorescence for this class of dyes increases when the viscosity of the environment increases, because the rotational freedom is restricted.⁷ A strong dispersion force associated with the high polarizability of the chromophoric chain favors aggregation of cyanine dyes in aqueous solution. The high dielectric constant of water facilitates the aggregation process by reducing the electrostatic repulsion between similarly charged dye molecules. Aggregation of these dyes occurs also in mixed solvents and in heterogeneous media, e.g., micelles. On the other hand, aggregation produces new spectral bands, now commonly referred as the *J* and the *H* band.^{8,9} *H* aggregates are spectroscopic entities that are characterized by a blue-shifted absorption band with respect to monomer absorption, whereas *J* aggregates present a red-shifted band. *H* aggregates appear at low concentration prior to the formation of the *J* aggregates. Until now, their physical size and structure have been controversial. It has not been clarified experimentally whether they really represent dimers, as commonly assumed, or whether they represent particles of mesoscopic size, which upon increase of the concentration further assemble to eventually form *J* aggregates.⁹

Pinacyanol (1,1'-diethyl-2,2'-carbocyanine) chloride (PIN) is a cationic dye belonging to the class of conjugated cyanine dyes that, because of its amphipathic nature, is soluble in a wide range of solvents including water and chloroform. The visible absorption spectrum of PIN consists of three overlapping spectral components, with the most intense band red-shifted relative to the others. In water, maxima of such spectral

components can be located at 600, 550, and ≈ 520 nm. The first one is usually interpreted as the vibrationless electronic $S_0 \rightarrow S_1$ transition and the other two as the same electronic transition under vibration cooperation. With increasing dye concentration, the spectrum undergoes some variations: the peak at 600 nm diminishes, whereas that at 550 nm enhances. In determined circumstances, such as the dye being absorbed on colloidal surfaces, these bands decrease with simultaneous appearance of a new absorption band at 495 nm.^{10,11} This latter band should correspond to the *H* band. The origin of such changes is the existence of aggregate forms of PIN (dimers, trimers, and higher aggregates). Because the dimer exists always in equilibrium with the monomer, the observed absorption spectrum, even at low dye concentrations, is a superposition of the spectra of the monomer and the dimer.

It is well-known that the local microenvironment surrounding a dye molecule influences its electronic structure and thus its photophysics. Changes in this local microenvironment, as the dye interacts with other species in solution, can produce measurable spectral shifts which can, in turn, be monitored spectroscopically.¹² This property, known as solvatochromism, allows elucidation of the influence of the immediate environment of the molecule within the probed system and, moreover, gives evidence of specific interactions. Differences in local polarizability might account for the spectral shifts of PIN in micellar media, because of the presence or absence of water. Hence PIN can function as a probe for local polarizability. Solvatochromism is caused by the differential solvation of the ground and first excited state of the chromophore.¹³ For instance, a reduction of the polarity of the medium produces bathochromic shifts of peaks of maximal absorption of PIN. This means that the ground-state molecule of PIN is better stabilized by solvation than the molecule in the excited state. In these circumstances, it is said that a "negative" solvatochromism is present.

Surfactants (above or below their critical micellar concentrations) affect the electronic absorption spectra of solutions of many dyes.^{14–16} Hence, spectroscopic techniques can be used

* To whom correspondence should be addressed. Fax: + 34 93 403 59 87. Phone: + 34.93.402.45.59. E-mail: estelric@farmacia.far.ub.es.

to determine certain physicochemical properties of micelles and vesicles.¹⁷ In previous works, the location of PIN in micelles of some trimethylammonium bromide surfactants was studied spectroscopically and by acid–base equilibrium. Results suggested the possibility of a cation– π interaction between the uncharged ring system of the dye and the cationic headgroups of the surfactants. On the other hand, curve-fitting techniques were applied in order to obtain the dimerization constant, as well as to decompose and analyze the absorption spectrum in terms of its component bands.^{18–19}

In the present work, we aim to elucidate the effects of the interaction of PIN with nonionic, cationic, and anionic surfactants, at micellar concentrations, by means of UV absorption spectroscopy. Our other objective is to determine the solubilization site of PIN in each micellar system as a function of the structure of the surfactant (charge and length of the hydrophobic tail).

2. Experimental Section

2.1. Materials. PIN and Triton X-100 (TX-100) were obtained from Sigma (St. Louis, MO); pyrene, *n*-hexadecyltrimethylammonium bromide C₁₆H₄₂NBr (HTAB), *n*-tetradecyltrimethylammonium bromide C₁₄H₃₈NBr (TTAB), *n*-dodecyltrimethylammonium bromide C₁₂H₂₅NBr (DTAB), and sodium dodecyl sulfate C₁₂H₂₅OSO₃[–]Na⁺ (SDS) were obtained from Fluka (Buchs, Switzerland); 1-dodecylpyridinium chloride hydrate 98% was from Aldrich (Steinheim, Germany). Organic solvents, when possible of spectroscopic grade, were purchased from Merck (Darmstadt, Germany). Solutions were made in double-distilled water purified through a Milli-Q system (Millipore, USA).

2.2. Procedure to Prepare Solutions. Stock solutions of PIN were made in CHCl₃. When necessary, the required amount was placed in a round-bottomed flask and evaporated at reduced pressure. To remove CHCl₃ traces, the residue was freeze-dried overnight and the appropriate solution was prepared. All PIN preparations were kept in the dark and wrapped in aluminum foil to lower the likelihood of photodecomposition during storage. To minimize dye adsorption, glassware and cuvettes were silanated with 2% (v:v) dichloromethylsilane/toluene solution and then rinsed with methanol.

2.3. Critical Micellar Concentration Determination. Critical micellar concentrations of cationic micelles and SDS micelles were measured with a Crison micro CN 2202 (Crison, Spain) conductivity meter, using a cell constant of 1.0 cm^{–1} and calibrated with KCl solutions in the appropriate concentration range. The errors in the conductance measurements were $\pm 0.50\%$. The surfactant solution was progressively added with a Hamilton microsyringe to water kept in a bath to maintain the temperature at 25 ± 0.5 °C, and the conductance was measured after thorough mixing and temperature equilibrium. The cmc of TX-100 was determined at the same temperature by the ring method²⁰ using a digital tensiometer (Processor Tensiometer K-12, Kr ss, Hamburg, Germany), which directly determines the real surface tension values at equilibrium.

2.4. Determination of Micellar Aggregation Numbers. Aggregation numbers of ionic micelles were determined by fluorescence quenching.²¹ The method involves labeling micelles with a fluorescent probe and measuring steady-state fluorescence before and after addition of a second species, the quencher, which deactivates excited molecules of the probe species. The probe used was pyrene, and the quencher was the dodecylpyridinium ion. According to this model, the aggregation numbers can be calculated by use of eqs 1 and 2

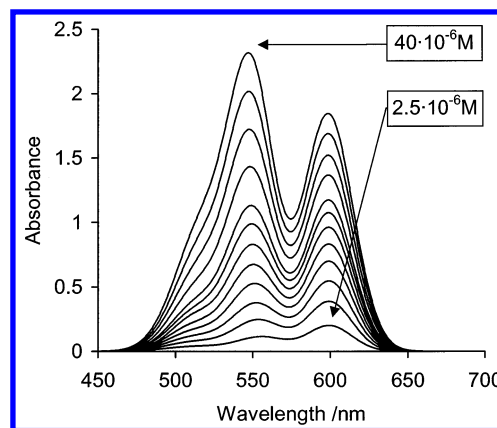


Figure 1. Concentration change in the visible absorption spectrum of PIN in water at 25 °C.

$$\ln \frac{I_0}{I_Q} = \frac{Q_{\text{mic}}}{M} \quad (1)$$

where I_0 is the emission intensity at a certain wavelength in the absence of an added fluorescence quencher, I_Q the intensity at the same wavelength at quencher concentration Q_{mic} , and M the concentration of micelles in solution. This concentration is related to the average aggregation number, N , the total surfactant concentration, S , and the cmc through eq 6, and eq 11 becomes

$$\ln \frac{I_0}{I_Q} = \frac{Q_{\text{mic}} N}{S - \text{cmc}} \quad (2)$$

If the fluorescence intensity at various quencher concentrations with fixed surfactant concentrations is measured, the aggregation number can be calculated from the slope of the straight line obtained by plotting $\ln(I_0/I_Q)$ against Q_{mic} , provided that the cmc is known.

2.5. Spectroscopic Measurements. The absorption spectra were recorded with a Shimadzu UV-2401 PC UV–visible spectrophotometer (Shimadzu, Japan) using a matched pair of glass cuvettes of 1 cm optical length placed in a thermostated cell holder, at 25 ± 0.1 °C. Spectra were fitted to three overlapping Gaussian curves with the help of a Gaussian curve fitting program that made it possible to obtain the amplitude, center, bandwidth at half of the maximum amplitude, and area of each Gaussian function.

3. Results and Discussion

The shape of the visible absorption spectrum of PIN in water was dependent on the dye concentration, as we can see in Figure 1. At low concentrations, band absorption at 600 nm predominated slightly over that observed at ≈ 558 nm, whereas in more concentrated solutions, this later was clearly higher than the most red-shifted band. This fact provoked a lack of linearity in the plot of absorbance vs dye concentration; that is, the Lambert–Beer law did not hold, as a consequence of the presence of monomer molecules of PIN, as well as its dimer form. We found elsewhere that the dimerization constant, K_D , is $(350 \pm 5) \times 10^2 \text{ M}^{-1}$.¹⁹ At any PIN concentration, the concentration of dimer (C_D) and monomer (C_M) species can be calculated from the experimental absorbances, $A(\lambda)$, the dimerization constant, and the molar absorptivities associated with both species, $\epsilon_M(\lambda)$ and $\epsilon_D(\lambda)$, respectively, according to the following equations:

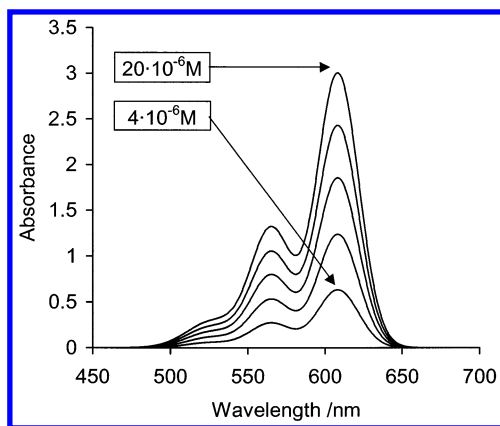


Figure 2. Visible absorption spectrum of PIN at different concentrations in 1-propanol at 25 °C.

TABLE 1: Shifts of the Wavelength of Maximal Absorption of PIN in Several Organic Solvents in Relation to the Maximal Absorption in Water

| solvent | $\Delta\lambda_{\text{max}}/\text{nm}$ | $E_T/\text{kJ mol}^{-1}$ | E_T^N |
|----------------|----------------------------------------|--------------------------|---------|
| water | 0 | 199.69 | 1 |
| methanol | 4.61 | 198.19 | 0.69 |
| ethanol | 7.32 | 197.30 | 0.50 |
| 1-propanol | 9.23 | 196.69 | 0.37 |
| 1-butanol | 10.50 | 196.28 | 0.29 |
| 1-octanol | 13.33 | 195.37 | 0.10 |
| acetone | 6.61 | 197.55 | 0.55 |
| DMSO | 14.80 | 194.91 | 0 |
| chloroform | 12.28 | 195.69 | 0.16 |
| benzyl alcohol | 17.52 | 194.04 | -0.18 |

$$K_D = C_D/C_M^2 \quad (3)$$

$$A(\lambda) = \epsilon_M(\lambda)C_M + \epsilon_D(\lambda)C_D \quad (4)$$

The transfer of the dye from bulk water to an organic phase affects its physicochemical properties, namely, its absorption spectrum. In this way, the spectral behavior was completely different when PIN was dissolved in organic solvents. In these cases, a regular increase of the maximal absorbance in both peaks was observed, and the Lambert–Beer was accomplished in the concentration range used. Another important feature observed was that both peaks underwent a bathochromic shift, more evident in the case of the peak near 600 nm. Figure 2 shows spectra of PIN at several concentrations in 1-propanol. Such spectra were qualitatively similar to those obtained with other nonaqueous solvents.

Table 1 shows the wavelength shifts of the maximal absorption of PIN in organic solvents in relation to the absorption near 600 nm of PIN in water. Moreover, the wavelength of maximal absorbance allowed calculating the molar electronic transition energies (E_T) of PIN in each one of the solvents used. E_T values, expressed as $\text{kJ}\cdot\text{mol}^{-1}$ were obtained from

$$E_T = hcN_A/\lambda_{\text{max}} = 119.6 \times 10^3/\lambda_{\text{max}} (\text{nm}) \quad (5)$$

where h is the Planck constant, c is the vacuum light velocity, and N_A is the Avogadro's constant. Differences between E_T values for PIN in water and in any of the organic solvents point out the variation in energy in the transference process from water to organic phase. The fact that such differences were always negative indicates that PIN solubilizes better in organic solvents than in water.

To make the results for the solvents readily comparable, the corresponding E_T were converted to a dimensionless, normalized

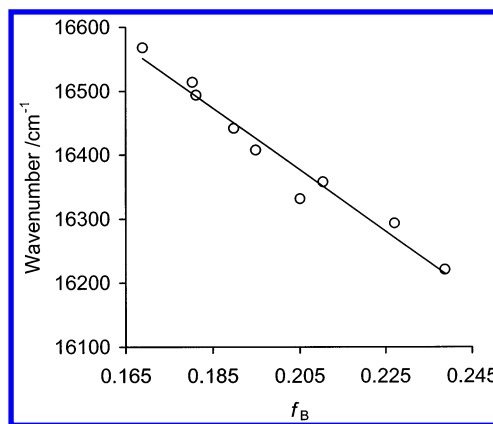


Figure 3. Bayliss graph for PIN. Solvents used are from left to right: methanol, acetone, ethanol, 1-propanol, 1-butanol, chloroform, 1-octanol, DMSO, and benzyl alcohol.

polarity scale, E_T^N , whose value for any solvent is defined according to eq 6, using water and dimethyl sulfoxide (DMSO) as extreme polar and nonpolar reference solvents, respectively

$$E_T^N = \frac{E_T(\text{solvent}) - E_T(\text{DMSO})}{E_T(\text{water}) - E_T(\text{DMSO})} \quad (6)$$

Hence, the E_T^N scale can range from 0.00 for DMSO to 1.00 for water, the most polar solvent. Negative values are obtained with solvents more apolar than DMSO, e.g., with benzyl alcohol.

There exists a direct relation between the wavenumber of maximal absorbance and the Bayliss function, f_B , of the refractive index, n_s of the solvent (eq 7):

$$f_B = \frac{n_s^2 - 1}{2n_s^2 + 1} \quad (7)$$

Figure 3 shows a plot of the absorption maximal of PIN as a function of the Bayliss function. Because of the dimerization of PIN in water, this value ($16\,678\text{ cm}^{-1}$ for $f_B = 0.170$) did not fit to the straight line, and for this reason, this datum was discharged.

Previous to the study of the interaction of PIN with micellar solutions, it was necessary to determine the critical micellar concentration (cmc) of each surfactant and the aggregation numbers (N) for the different surfactant concentrations. For nonionic micelles, a value of 112 was assumed as N , irrespective of the concentration. Table 2 summarizes the values of cmc obtained experimentally and the parameters of the linear regression that allow calculation of N for each surfactant at any concentration. The length of the hydrophobic tail of the alkyltrimethylammonium bromide surfactants affects some properties of the micelles; for example, a decrease in the length increases the cmc, and the degree of micelle dissociation decreases the micellar aggregation number and the thickness of its Stern layer. As a result, the dodecyl chain micelles are smaller and less compact and their Stern layers are more ionic than their cethyl (HTAB) chain counterpart.

The interaction of micellar systems with PIN was studied at a constant dye concentration (10^{-5} M) and at variable surfactant concentrations. In every case, the ratio surfactant/dye was at least 1000. PIN may be adsorbed on the surface oriented near the surface (short penetration) or may be trapped in the hydrocarbon core (deep penetration). Moreover, the interaction (or solubilization) is a dynamic equilibrium process, and the

TABLE 2: Values of Several Parameters of the Micellar Systems Studied^a

| | surfactant | | | | |
|-------------------------------------------------------------------|-----------------------------------------------|-----------------------------------------------|------------------------------------------------|-----------------------------------------------|--------|
| | DTAB | TTAB | CTAB | SDS | TX-100 |
| cmc/mM | 15.50 | 3.89 | 0.89 | 8.00 | 0.27 |
| parameters of linear regression | $N = 59.61 + 0.0582[S]$ ($r^2 = 0.9917$) | $N = 74.05 + 0.1869[S]$ ($r^2 = 0.9974$) | $N = 105.40 + 0.4028[S]$ ($r^2 = 0.9969$) | $N = 55.64 + 0.1187[S]$ ($r^2 = 0.9946$) | 112 |
| $K_A/10^3 \text{ M}^{-1}$ | 7.88 | 9.34 | 10.77 | 1117.45 | 418.99 |
| $\lambda_{\text{mic}}/\text{nm}$ | 612.57 | 613.39 | 614.36 | 607.25 | 610.49 |
| $\lambda_{\text{isos}}/\text{nm}$ | 561.72 | 562.31 | 562.69 | 558.48 | 599.37 |
| $\epsilon_{\text{isos}}/10^3 \text{ M}^{-1} \cdot \text{cm}^{-1}$ | 7.88 | 9.34 | 10.77 | 1117.45 | 418.99 |
| $\Delta\lambda_{\text{max}}/\text{nm}$ | 13.51 | 14.33 | 15.30 | 8.19 | 11.43 |
| $E_T/\text{kJ} \cdot \text{mol}^{-1}$ | 195.29 | 195.03 | 194.72 | 197.00 | 195.95 |
| E_T^N | 0.08 | 0.02 | -0.04 | 0.43 | 0.22 |
| $\Delta G/\text{kJ} \cdot \text{mol}^{-1}$ | -22.23 | -22.65 | -23.00 | -34.51 | -32.08 |

^a cmc, critical micellar concentration; K_A , association constant; λ_{mic} , wavelength in which the maximal amount of PIN is into the micelles; λ_{isos} , the isosbestic point obtained with the several micellar concentrations; ϵ_{isos} , the molar absorptivity at the isosbestic point; $\Delta\lambda_{\text{max}}$, shift of the wavelength of maximal absorption of PIN in relation to the maximal absorption in water; E_T , molar electronic transition energy; E_T^N , normalized molar electronic transition energy; and ΔG , free energy change. The concentration of surfactant, $[S]$, is expressed as mmol L⁻¹.

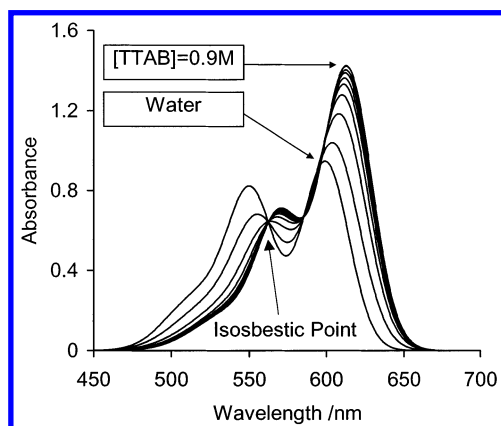


Figure 4. Visible absorption spectrum of 10^{-5} M PIN in several concentrations of TTAB (from 0.01 to 0.09 M) at 25 °C.

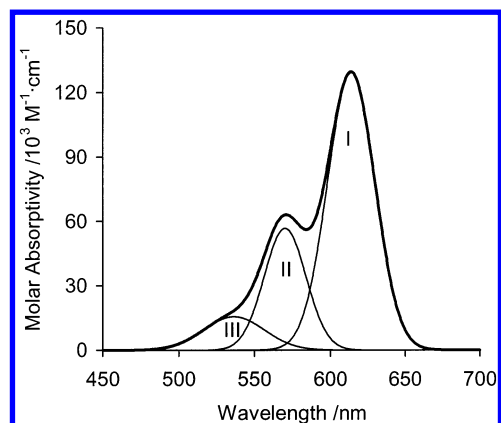


Figure 5. Deconvolution of spectrum of PIN (10^{-5} M) in micelles of TTAB. Deconvolution was performed assuming a logarithmic-normal profile of the spectrum.

solubilize may spend different residence times at different levels between the core and the surface. Figure 4 presents the absorption spectra of PIN in micelles of TTAB at surfactant concentrations ranging from 0 (PIN dissolved in water) to 0.09 M. The absorption of the most red-shifted peak increased when the surfactant concentration increased to 0.04. Above this, the absorption seemed to have reached a maximum. The increase in absorbance values at increasing surfactant concentrations indicates that a larger number of the dye molecules are taken up by TTAB micelles. Concomitant to this hyperchromic effect, the surfactant-dye interaction resulted in a bathochromic shift of the highest band. The lower peak also underwent a shift to

TABLE 3: Amplitude (Molar Absorptivity) and Center (λ_{max}) of the Bands Obtained from Gaussian Curve Fitting Analysis of the Absorption Spectra of the PIN in Micelles (Monomeric Form) and in Water (Monomeric and Dimeric Forms)

| | $\epsilon/\text{M}^{-1} \text{ cm}^{-1}$ | $\lambda_{\text{max}}/\text{nm}$ |
|----------------|------------------------------------------|----------------------------------|
| water | | |
| monomeric form | | |
| band I | 94 400 | 599.8 |
| band II | 46 000 | 557.9 |
| band III | 12 500 | 509.9 |
| dimeric form | | |
| band I | 26 400 | 593.4 |
| band II | 129 700 | 546.6 |
| band III | 75 400 | 522.0 |
| surfactants | | |
| DTAB | | |
| band I | 127 800 | 612.5 |
| band II | 57 100 | 568.7 |
| band III | 15 400 | 534.1 |
| TTAB | | |
| band I | 131 100 | 614.0 |
| band II | 57 600 | 570.2 |
| band III | 15 800 | 536.5 |
| CTAB | | |
| band I | 134 600 | 615.1 |
| band II | 61 500 | 570.7 |
| band III | 15 200 | 533.8 |
| SDS | | |
| band I | 150 300 | 607.9 |
| band II | 62 300 | 564.6 |
| band III | 12 800 | 525.5 |
| TX-100 | | |
| band I | 148 600 | 611.2 |
| band II | 63 900 | 567.5 |
| band III | 14 000 | 528.8 |

the red, but then the corresponding absorbance decreased. A sharp isosbestic point at $562.3 \pm 0.2 \text{ nm}$ with $\epsilon = 43.5 \times 10^3 \text{ M}^{-1} \text{ cm}^{-1}$ was found; it points to an equilibrium between two spectrophotometrically distinguishable states of PIN, namely, PIN in bulk water and in the micellar pseudo phase.²² Similar behavior was observed with the other four surfactants. Values of the remaining isosbestic points and the associated molar absorptivity are displayed in Table 2. The shift to the red associated with PIN on addition of surfactants and enhancement of absorbance indicates the passage of the chromophore from polar aqueous medium to a relatively nonpolar site in micellar environment. Deconvolution of each one of these spectra afforded three Gaussian bands (Figure 5), which sum reconstructed the original spectrum. Table 3 displays the values of the wavelength of maximal absorption and molar absorptivity

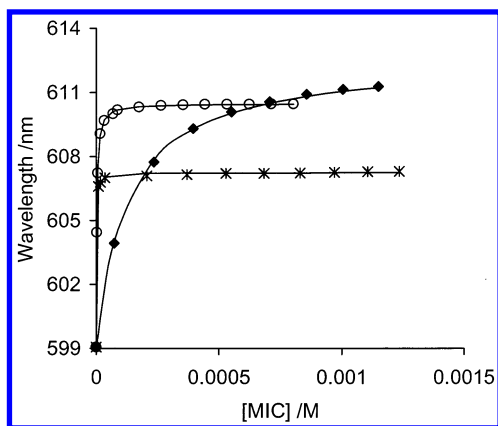


Figure 6. Variation of the wavelength of maximal absorption as a function of micellar concentration for negative (SDS, *), positive (DTAB, ♦) and nonionic (TX-100, ○) micelles.

of the bands for each surfactant. As stated elsewhere, PIN incorporates into a micelle as a monomer.¹⁹

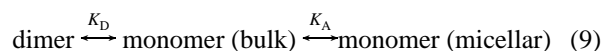
The concentration of micelles, M , is obtained from

$$M = \frac{S - \text{cmc}}{N} \quad (8)$$

where S is the surfactant concentration and N is the aggregation number.

The variation of the wavelength of maximal absorption as a function of micelle concentration, M , is displayed in Figure 6. For simplification, only curve achieved with DTAB, as example of cationic micelles, is shown, but the interaction with the other cationic micelles followed similar trends. We can observe a different behavior depending on the kind of micelle. Negative micelles reached the maximal wavelength shift; that means that the interaction was complete at a very low micellar concentration. In this case the driving forces are both hydrophobic and Coulombic interactions between the negative micelle and the positive dye. This interaction was strong even at submicellar surfactant concentrations (data not shown), because of the formation of ion pairs between the monomeric dye and the molecule of SDS. Nonionic micelles interacted also at low micellar concentrations. It has been suggested that the interaction between a cationic dye and nonionic micelles is a charge-transfer interaction.²³ In this case, the poly(ethylene oxide) residues of TX-100 are more favorable for the location of a dye cation, because they act as electron donors. The characteristics of the interaction of DTAB and the other cationic micelles were different. The shift of wavelength was gradual, and at the highest micellar concentrations used, the maximal value was still not achieved. It is claimed that PIN interacts with cationic micelles by means of the attraction of the noncharged aromatic quinoxaline ring present in the dye with the cationic headgroups of these surfactants on the micellar surface, that is, by means of a cation- π interaction.¹⁹

As said above, PIN incorporates into the micelle as a monomer. Now, it is plausible to suppose the existence of a new equilibrium



Therefore, the presence of micelles produces a shift to the right, and the conversion of monomer into dimers at increasing DTAB (and other cationic surfactants) concentrations was less extensive than for nonionic and anionic surfactants.

Because dye molecules are distributed between bulk solvent and micellar phases, the corresponding equilibrium is given by the micelle association constant, K_A , which is calculated from the following equation:²⁴

$$\lambda_{\text{obs}} = \lambda_w + \frac{\lambda_{\text{mic}} - \lambda_w}{\frac{1}{K_A(M)^n} + 1} \quad (10)$$

where λ_{obs} is the wavelength of maximal absorption observed at a micellar concentration, M ; λ_w and λ_{mic} are the wavelengths of maximal absorption of PIN in the absence of surfactant and when the maximal amount of PIN is into the micelles, respectively; and n is the number of monomers of the dye associated with the micelle.

A nonlinear curve fitting of λ_{obs} vs M afforded the values of the association constant and the λ_{mic} . The value of n was in all of the cases ≈ 1 ; this corroborated that the maximum number of dye molecules that each micelle can accommodate is one.

Table 2 shows the values of the association constant and the wavelength at which the maximal amount of PIN is into the micelles. The extremely high value of the association constant obtained from the interaction of SDS micelles and PIN allows us to anticipate that, in the presence of these micelles, the majority of the PIN present will be associated. The binding properties of the cationic dyes are of intrinsic interest because their binding to SDS has both an electrostatic and a hydrophobic component. The Menger micelle model predicts the distribution of cationic dye in a large region surrounding the relatively small hydrophobic core.²⁵ In cationic micelles, the K_A value increases with increasing chain length.

Values of λ_{mic} made it possible to determine the shift of wavelength in relation to the water and, from this, to calculate the molar and the normalized electronic transition energies of PIN in the micellar systems. On the other hand, the association constant afforded the free energy change ($\Delta G = -RT \ln K_A$; Table 2). Concerning this last parameter, negative values of ΔG point out the spontaneity of the micellization of the dye.

Once the K_A value is known, it is possible to calculate the fraction of micellized (f_{mic}) and nonmicellized (f_w) PIN from

$$f_{\text{mic}} = \frac{K_A[M]}{1 + K_A[M]} \quad (11)$$

$$f_w = \frac{1}{1 + K_A[M]} \quad (12)$$

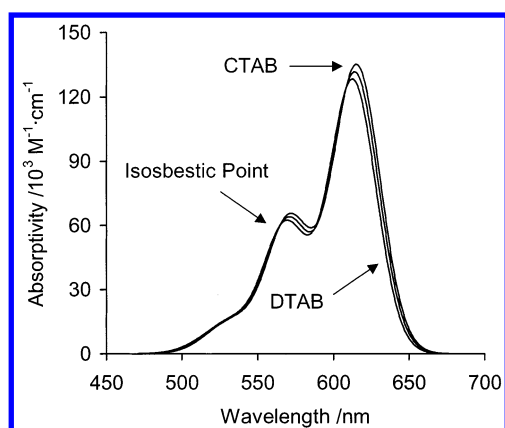
respectively.

The values of micellar fraction of PIN are listed in Table 4. The nonmicellized PIN is the amount of dye molecules present in the bulk solution, in a proportion between monomers and dimers that can be determined by the dimerization constant, K_D . Values of f_{mic} are well correlated with the molar electronic transition energies ($r > 0.994$ for any micellar system).

The hydrophobic group present in the PIN molecules is able to pull the molecule to the hydrophobic core of a micelle. Because of this pulling effect, the hydrophilic part of the molecule is localized at various regions of the micelles. To know which is the environment of PIN in the micelles, or in other words which is the location of micellar PIN, values of the wavenumber corresponding to λ_{mic} were related to the refraction index by interpolating into the straight line displayed in Figure 3. In this way, PIN experienced a refractive index of 1.463 in DTAB, of 1.474 in TTAB, of 1.494 in HTAB, of 1.375 in SDS,

TABLE 4: Fraction of Micellized PIN at Various Micellar Concentrations for the Five Surfactant Systems Studied

| micellar conc/ M 10 ³ | f_{mic} | | | | |
|-------------------------------------|------------------|-------|-------|-------|--------|
| | DTAB | TTAB | CTAB | SDS | TX-100 |
| 0.0005 | | | | | 0.462 |
| 0.0010 | | | | | 0.732 |
| 0.0020 | | | | | 0.866 |
| 0.0040 | | | | | 0.933 |
| 0.0080 | | | | | 0.967 |
| 0.0085 | | | | 0.908 | |
| 0.0090 | | | | 0.952 | |
| 0.0100 | | 0.429 | 0.473 | 0.975 | 0.973 |
| 0.0200 | 0.368 | 0.659 | 0.645 | 0.996 | 0.987 |
| 0.0300 | 0.651 | 0.754 | 0.727 | 0.998 | 0.991 |
| 0.0400 | 0.757 | 0.805 | 0.776 | 0.998 | 0.993 |
| 0.0500 | 0.813 | 0.838 | 0.808 | 0.999 | 0.995 |
| 0.0600 | 0.847 | 0.860 | 0.831 | 0.999 | 0.996 |
| 0.0700 | 0.871 | 0.876 | 0.848 | 0.999 | 0.996 |
| 0.0800 | 0.888 | 0.889 | 0.861 | 0.999 | 0.997 |
| 0.0900 | 0.900 | 0.898 | 0.871 | 0.999 | 0.997 |

**Figure 7.** Spectra of PIN in cationic micelles: CTAB (upper spectrum), TTAB (middle spectrum), and DTAB (lower spectrum).

and of 1.427 in TX-100 micelles. Thus, the immediate micro-environment of the chromophore of PIN in SDS micelles is midway between 1-propanol and ethanol. In nonanionic micelles, PIN is in a 1-octanol-like environment. The more hydrophobic location is assigned to cationic micelles in which PIN finds a medium that ranges from chloroform to DMSO. That means that PIN is incorporated near the dry core of the micelle.

Results described above suggest that the interaction of PIN with micellar systems depends on the hydrocarbon chain as well as on the headgroup. To check the influence of the hydrocarbon chain, spectra of PIN in the three cationic systems were depicted (Figure 7). Spectra were qualitatively similar, although slight quantitative differences can be observed. The value of maximal absorbance is related to the number of methyl groups. In this way, HTAB, with a chain of 16 methyl, gave the highest value, whereas the least corresponded to DTAB with 12 methyl. That means that the more hydrophobic the molecule, the higher the hyperchromic effect produced. Similar features can be observed when PIN is dissolved in a series of *n*-alcohols (data not shown). It is remarkable to indicate the presence of an isosbestic point at 564.8 nm. These findings are inverse but equivalent to that observed in the interaction of surfactants with cyanines of different lengths of alkyl chain.²⁶ The longer the hydrophobic alkyl chain of the dyes, the deeper is their penetration into the hydrophobic interior of the micelle, and the less polar the solubilization site. As for the headgroup, the association of PIN to micelles followed this order: anionic \gg nonionic \gg cationic (Table 2). The shift of wavelength of

maximal absorption was also related with the headgroup: cationic $>$ nonionic $>$ anionic (Table 2). However, the hyperchromic effect undergone by the highest peak was bigger in anionic micelles than in nonionic and cationic ones (Table 3).

4. Summary

The results presented in this study have shown that the transfer of pinacyanol from bulk water to organic phases or micellar systems affects its spectral properties leading to bathochromic shifts of the main spectral peaks. Such shifts were interpreted as the passage of the dye chromophore from a polar aqueous medium to a relatively nonpolar site in the micellar environment. The presence of a sharp isosbestic point indicated an equilibrium between two spectrophotometrically distinguishable states of PIN, namely, PIN in bulk water and in micellar pseudophase. Negative micelles produced the maximal interaction, and, in this case, the driving forces were both hydrophobic and Coulombic interactions. The interaction of the dye with positive micelles was interpreted as a cation- π interaction. Finally, the interaction with nonionic micelles was thought to be a charge transfer, because the poly(ethylene oxide) residues can easily act as electron donors. Changes in the wavelength of maximal absorption of PIN as a function of micellar concentration allowed us to quantify this interaction by means of the association constants. The extremely high value of the association constant of PIN to SDS micelles permitted us to affirm that the dye was almost completely associated to micelles. On the other hand, the results showed that the number of dye molecules that each micelle can accommodate was one. The location of PIN into the micelles depends on the hydrocarbon chain as well as on the surfactant headgroup.

Acknowledgment. R.S. is a recipient of a grant from the Generalitat de Catalunya (FI 00337 UB).

References and Notes

- (1) Kaschny, P.; Goñi, F. M. *Eur. J. Biochem.* **1992**, *207*, 1085.
- (2) Kaschny, P.; Goñi, F. M. *J. Colloid Interface Sci.* **1993**, *160*, 24.
- (3) Pramanick, D.; Mukherjee, D. *J. Colloid Interface Sci.* **1993**, *157*, 131.
- (4) González Mañas, J. M.; Kaschny, P.; Goñi, F. M. *J. Phys. Chem.* **1994**, *98*, 10650.
- (5) Bernik, D. L.; Disalvo, E. A. *Chem. Phys. Lipids* **1996**, *82*, 111.
- (6) Murphy, S.; Schuster, G. B. *J. Phys. Chem.* **1995**, *99*, 8516.
- (7) Van der Auweraer, M.; Van den Zegel, M.; Boens, N.; De Schryver, F. C.; Willig, F. *J. Phys. Chem.* **1986**, *90*, 1169.
- (8) Barazzouk, S.; Lee, H.; Hotchandani, S.; Kamat, P. V. *J. Phys. Chem. B* **2000**, *104*, 3616.
- (9) Von Berlepsch, H.; Böttcher, C. *J. Phys. Chem. B* **2002**, *106*, 3146.
- (10) Horng, M. L.; Quitevis, E. L. *J. Chem. Educ.* **2000**, *77*, 637.
- (11) Mitra, A.; Nath, R. K.; Chakraborty, A. K. *Colloid Polym. Sci.* **1993**, *271*, 1042.
- (12) Von Wandruszka, R. *CRC Crit. Rev. Anal. Chem.* **1992**, *23*, 187.
- (13) Reichardt, C. *Chem. Rev.* **1994**, *94*, 2319.
- (14) Zachariasse, K. A.; Van Phuc, N.; Kozankiewicz, B. *J. Phys. Chem.* **1981**, *85*, 2676.
- (15) Drummond, C. J.; Grieser, F.; Healy, T. W. *Faraday Discuss. Chem. Soc.* **1986**, *81*, 95.
- (16) Sarkar, M.; Poddar, S. *J. Colloid Interface Sci.* **2001**, *221*, 181.
- (17) Zana, R. *Surfactant Solutions: New Methods of Investigation*; Marcel Dekker: New York, 1987.
- (18) Sabaté, R.; Gallardo, M.; Estelrich, J. *J. Colloid Interface Sci.* **2001**, *233*, 205.
- (19) Sabaté, R.; Gallardo, M.; De la Maza, A.; Estelrich, J. *Langmuir* **2001**, *17*, 6433.
- (20) Lunkenheimer, K.; Wantke, D. *Colloid Polym. Sci.* **1981**, *259*, 354.
- (21) Turro, N. J.; Yekta, A. *J. Am. Chem. Soc.* **1978**, *100*, 5951.
- (22) Qi, L.; Ma, J. *J. Colloid Interface Sci.* **1998**, *197*, 36.
- (23) Sarkar, M.; Poddar, S. *Spectrochim. Acta A* **1999**, *55*, 1737.
- (24) Novaki, N. P.; El Seoud, O. A. *Langmuir* **2000**, *16*, 35.
- (25) Menger, F. M.; Doll, D. W. *J. Am. Chem. Soc.* **1984**, *106*, 1109.
- (26) Mishra, A.; Behera, R. K.; Mishra, B. K.; Behera, G. B. *J. Photochem. Photobiol. A* **1999**, *121*, 63.